Geochimica et Cosmochimica Acta Vol. 53, pp. 2113–2118

0016-7037/89/$3.00 + .00

LETTER

Anomalous quartz from the Roter Kamm impact crater, Namibia: Evidence for post-impact hydrothermal activity?

CHRISTIAN KOEBERL[1,2], KURT FREDRIKSSON[3], MICHAEL GÖTZINGER[4] AND WOLF UWE REIMOLD[5]

[1]Lunar and Planetary Institute, 3303 NASA Road One, Houston, TX 77058, U.S.A.
[2]Institute of Geochemistry, University of Vienna, Dr.-Karl-Lueger-Ring 1, A-1010 Vienna, Austria
[3]Department of Mineral Sciences, Smithsonian Institution, Washington, DC 20560, U.S.A.
[4]Institute of Mineralogy and Crystallography, University of Vienna, Dr.-Karl-Lueger-Ring 1, A-1010 Vienna, Austria
[5]Schonland Research Centre, University of the Witwatersrand, WITS 2050, Johannesburg, South Africa

(*Received April* 5, 1989; *accepted in revised form June* 21, 1989)

Abstract—Centimeter-sized quartz pebbles have been found on the rim of the Roter Kamm impact crater. The Roter Kamm crater has a diameter of about 2.5 km and is situated in the Namib Desert, SWA/Namibia. Because of the sand coverage, impact products (breccias, impact melt, shocked rocks) are exposed exclusively in the form of ejecta on the crater rim. The quartz pebbles were found close to the main deposits of the impact breccias and show signs of wind abrasion. Thin sections revealed that the pebbles consist of individual quartz domains that are up to 1 mm in size. Under crossed nicols (polarized light), all individual domains show extinction almost simultaneously within ±2°, which is a rare phenomenon. Microprobe studies, neutron activation analyses, and X-ray diffractometry confirmed that the material consists of pure quartz. The quartz contains three different types of fluid inclusions: primary inclusions (size about 5–10 μm) that record the formation conditions of the quartz, very small (<1 μm) secondary inclusions associated with the grain boundaries, and late inclusions of irregular size. Freezing point depression measurements of the primary inclusions indicate fluid salinities between 18.3 and 19.6 wt% NaCl. Homogenization temperatures (T_h) for the primary inclusions range from 165 to 250°C. The quartz and the primary inclusions may provide evidence for a post-impact phase of extensive hydrothermal activity, generated by the residual heat from the kinetic energy of the impact.

INTRODUCTION

THE ROTER KAMM crater is located in the Namib Desert (South West Africa/Namibia) at 27°46′S and 16°18′E. The crater is difficult to access and has been rarely visited by geologists. Earlier geological and geophysical work was reported by DIETZ (1965) and FUDALI (1973). Based on morphological studies (shape, appearance, and setting of the crater) and geophysical investigations (gravity and magnetic profiles), it was suggested by these authors that the circular depression is a hypervelocity impact crater. More recently, new field studies have been made during a number of small expeditions to the crater, and a large number of samples was collected and analyzed. The impact nature of the crater was confirmed by the discovery of impact breccias and associated shock metamorphic effects (multiple sets of planar features in quartz) as reported by MILLER and REIMOLD (1986), REIMOLD and MILLER (1987), and REIMOLD *et al.* (1988).

During a recent (1987) geological survey of the outcrops at the crater rim, two of the authors (C.K., W.U.R.) collected several conspicuous quartz samples. The quartz was found only at a few specific locations on the crater rim close to major occurrences of impact breccias, which are shown in Fig. 1. The quartz samples are centimeter-sized and of nonspherical shape. The general appearance and color (translucent, yellowish) is very similar to Libyan Desert Glass. Crystallographic, petrologic, and chemical studies have been performed to study the quartz. It was found that the quartz samples contain several types of fluid inclusions: primary (original) inclusions, very small secondary inclusions, and late-stage irregular inclusions.

Fluid inclusions in material associated with impact craters have rarely been studied. Recently BAIN and KISSIN (1988) studied fluid inclusions in the glassy phases of polymict breccias at the Haughton impact structure, Canada, and found that they are water-rich, have low salinity, and are CO_2-free. These inclusions were interpreted to have originated from the interaction of the silicate impact melts with superheated water immediately following the impact. KOMOR *et al.* (1988a,b) analyzed fluid inclusions in quartz from granite that was recovered from drill core samples at the Siljan impact structure, Sweden. They found that the fluid inclusions postdate the planar features in the quartz and interpreted them as being indicative of large-scale impact-generated hydrothermal activity below the crater. Evidence for hydrothermal activity has been found at other terrestrial impact craters, including Brent, Rochechouart, Clearwater, and the Ries Kessel (PHINNEY *et al.*, 1978; ALLEN *et al.*, 1982; NEWSOM *et al.*, 1987; REIMOLD *et al.*, 1987) and is postulated to be of great importance on Mars (NEWSOM, 1980; ALLEN *et al.*, 1982). The impact-induced hydrothermal activity at impact craters is an important phase of post-impact alteration and clearly deserves more attention than it has attracted in the past.

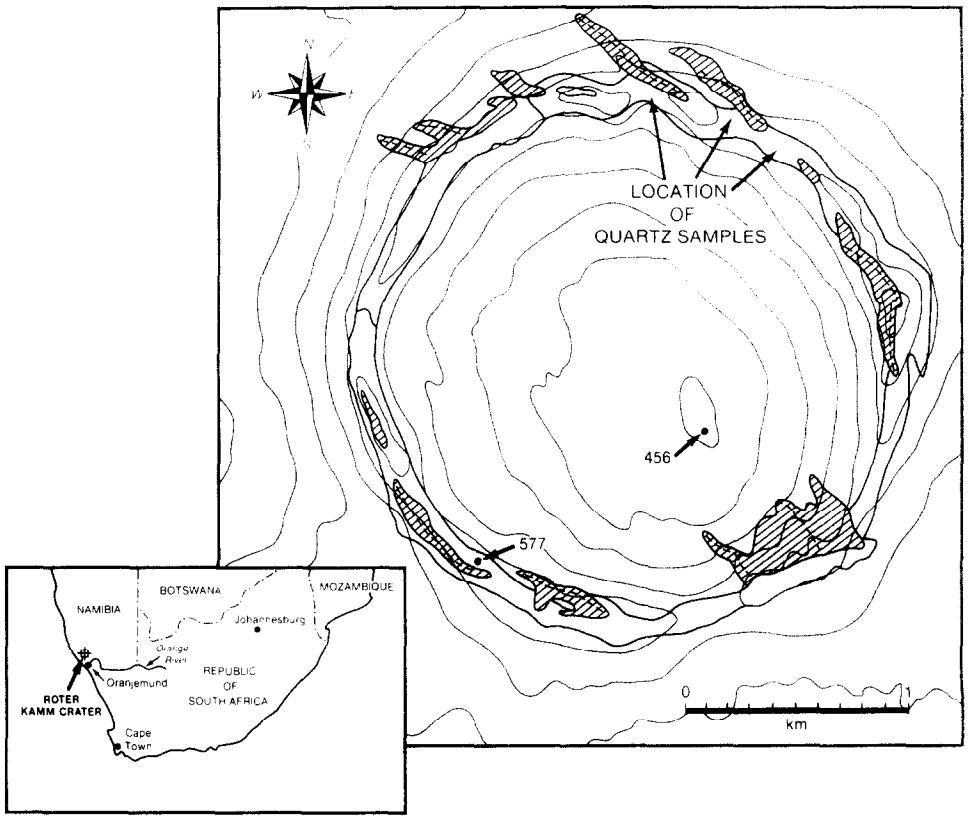

FIG. 1. Topography and structure of the Roter Kamm, Namibia, impact crater. The geographical location of the crater is shown in the inset. The shaded areas indicate coverage by (red; probably hematized) sand dunes. The contour interval is 20 meters, the topographic low and one topographic high at the crater rim are given in meters. The heavy lines indicate the boundaries of the crater rim as defined by orthogneisses and pegmatites (REIMOLD and MILLER, 1989). The crater floor and the surroundings of the crater are covered by post-impact erosional deposits, thus the only accessible impact deposits are located at the crater rim, which is an eroded feature too. The arrows indicate the general location where the quartz samples, that are described in this study, have been found. Numbers indicate elevations in meters. Modified after REIMOLD and MILLER (1989).

GEOLOGICAL SETTING OF THE ROTER KAMM CRATER

The Roter Kamm impact crater is located in the arid environment of the southern Namib Desert in Namibia. The crater has a rim crest diameter of about 2.5 km and the topographic difference between the highest point of the rim and the crater floor is 158 m (*i.e.*, apparent depth, caused by erosional infill). It has a rather narrow rim and shows a high degree of circularity. A map of the general location of the crater and of the crater structure is given in Fig. 1. A detailed account of the crater geology and current knowledge was recently provided by REIMOLD and MILLER (1989).

The magnetic profile (obtained with a field magnetometer) of the crater is featureless, while the gravity profile seems to show a negative residual gravity anomaly inside the crater (FUDALI, 1973). The shape and structure of the crater indicates that it is simple and bowl-shaped. The age of the crater is not known, but is thought to be less than 10 Ma (REIMOLD and MILLER, 1989).

The impact occurred in Precambrian granitic-granodioritic orthogneiss target rocks of the 1200–900 Ma old Namaqualand Metamorphic Complex. Arkose remnants on the rim and amphibolite xenoliths in the orthogneisses as well as quartz veins and quartz-feldspar pegmatites are common lithologies in the outcrop. Pegmatite fragments have been found together with impact melts and breccias along the crater rim. Graphitic schist was found as small fragments on the crater rim and may have been part of the surface lithology at the time of the impact (REIMOLD and MILLER, 1989). Today the crater floor is covered by aeolian sand deposits and broad shifting sand dunes of a characteristic red color that overlies an end-Miocene calcrete. Because of this erosional cover, the only impact-derived materials are exposed at the crater rim.

The orthogneisses forming the basement lithology have a composition that ranges from dioritic and granodioritic to granitic. Blackening of the feldspar is observed in the basement gneiss and in the pegmatites, which has been interpreted by REIMOLD and MILLER (1989) to have been caused by thermal breakdown of mafic minerals due to impact heating. Some basement rocks (collected at the crater rim) show signs of deformation (*e.g.*, fracturing, brecciation), but no characteristic petrographic shock effects have been found in them. Quartz pegmatites and quartz-feldspar-pegmatites were probably the second most common lithology in the target

area. The pegmatite shows similar deformation features as the gneissic basement rocks (REIMOLD and MILLER, 1989).

Pseudotachylite is found along the crater rim associated with gneiss or pegmatite, or in the form of allochthonous fragments. The pseudotachylite occurs as networks of millimeter-wide veinlets, or centimeter- to meter-thick dikes, or even larger zones with pseudotachylite as the major component (REIMOLD and MILLER, 1989). Pseudotachylite is thought to form *in situ* either by tectonic frictional melting, or by shock brecciation (SCHWARZMANN *et al.*, 1983), or by both processes. In the case of the Roter Kamm crater it seems reasonable to assume that it was formed due to extensional settling and adjustment of basement blocks during the impact in the late modification stage. Within some pegmatites, the pseudotachylite shows color variations indicating that, besides *in situ* melting, mixing of different melts may have occurred in some cases.

A large number of often bomb-shaped impact-melt breccias have been found along the northern part of the crater rim, in the same general locations where our quartz samples have been collected. The melt bombs have mostly a fine crystalline structure (probably because of recrystallization). Some contain clasts with shock deformation features (multiple sets of planar elements; diaplectic glass). The chemical composition of basement rocks, pseudotachylite, and melt breccias was studied by REIMOLD *et al.* (1988), REIMOLD and MILLER (1989), and BISHOP *et al.* (1989). Mixing models developed in these studies indicate that the melt breccias have been formed from pegmatite, schist, granite, and mafic-ultramafic components, with pegmatite being the main source. No cosmic component (bolide signature) has been identified in the impact melts so far (REIMOLD and MILLER, 1989; BISHOP *et al.*, 1989).

SAMPLES AND METHODS

About one dozen quartz samples have been collected at two adjacent locations in the northern part of the crater rim (Fig. 1). The samples have a non-spherical, sub-angular, chunky shape and are about 1–2 cm in size with a smooth surface. From three samples, several thin sections were cut for mineralogical and petrographic studies, plus one thick section for fluid-inclusion measurements. In addition, thin sections were prepared of quartz crystals from pegmatites found at the crater rim for comparison measurements (especially for fluid-inclusion studies). We have studied sections of a cloudy white crystal from pegmatite sample 87 E, and of a clear crystal from pegmatite sample RK 8704.

The ARL-SEMQ electron microprobe at the Department of Mineral Sciences, Smithsonian Institution, was used to check the purity of the quartz, and the mineralogy was confirmed with X-ray diffractometry at the Smithsonian Institution. Standard instrumental neutron activation analysis was used at the University of Vienna to determine if any minor elements are present at significant levels. The fluid inclusion measurements were made at the University of Vienna using a Linkam THM 600 heating and cooling stage with a PR 600 programmer, mounted on an Olympus BH-2 optical microscope. Transmission infrared spectra were recorded using a Perkin Elmer PE 580 B infrared spectrometer.

MINERALOGY AND CHEMISTRY

The X-ray diffractogram (performed on a powdered sample) shows that the material consists of pure quartz without any evidence of additional mineral phases. No line broadening or other difference from a quartz standard was found. The electron microprobe analyses confirmed the absence of any major elements in detectable quantities. A 50 mg chip was irradiated to determine the trace element content by neutron activation analysis. Except for Mn (3 ppm) and Na (5 ppm), trace element contents are not significant or are below the detection limit (*e.g.*, Sc, Cr, Co, REE below 0.1 × chondritic abundances). Infrared spectra were acquired using a 120 μm thick section (also used for fluid inclusion studies). No CO_2 peaks were detected, and the water content of the quartz (including the fluid inclusions) is 30 ppm, which is near the limit of detection of this method (THOMPSON, 1965).

Transmission infrared spectra of thin sections of quartz from pegmatites are different from the spectra obtained for the section of the quartz pebble. A spectrum obtained of a clouded white quartz from a pegmatite shows clear evidence for CO_2. The water content of this quartz (obtained by transmission IR spectroscopy of different sections) varies between 930 and 1240 ppm. The water content of clear translucent quartz crystals from pegmatites is about 100 ppm.

The thin sections were studied by optical microscopy and show the presence of individual domains (grains) of up to about 1 mm in size. These individual grains are structurally bound together and are visible only under crossed nicols. The determination of the crystal axis showed that the crystals are anomalously biaxial in the conoscopic image. The extinction behavior of the individual grains is very interesting. Under crossed nicols all individual quartz grains in each thin section extinguish virtually simultaneously. The range of extinction for all thin sections is within a maximum of ±2°. This is illustrated in Fig. 2a–d, which shows total extinction for all grains between 35.4 and 37.8° in a series of photos. A few larger areas show slight undulatory extinction. The reason for this behavior is not known, but may be associated with the formation of the quartz or the impact shock. No sign of shock metamorphism, however, is observed in the quartz pebbles. The size of the collected pebbles and the abundance of pegmatite in the basement may indicate that the quartz pebbles were derived from the pegmatite (*e.g.*, by recrystallization).

In order to compare the quartz pebbles to quartz from pegmatites, we studied sections of pegmatite quartz as well. The microscopic appearance of the pegmatite quartz in thin sections is very different from that of the quartz pebbles. The cloudy quartz shows a polycrystalline structure with numerous cracks and tiny fluid inclusions (<0.5 μm). The extinction under crossed nicols is undulatory, and the range of extinction is about 40°. The translucent quartz does not consist of individual domains like the quartz pebbles. It shows undulatory extinction over a range of about 35°, and contains very small (~1 μm length) needles of an unidentified mineral, perhaps tourmaline. Thus the optical characteristics of quartz from pegmatites are significantly different from those of the quartz pebbles.

FLUID INCLUSIONS

During the study of the thin sections at high magnifications we discovered several generations of fluid inclusions within the quartz samples. Three varieties can be distinguished. Primary two-phase, liquid-vapor fluid inclusions are shaped as

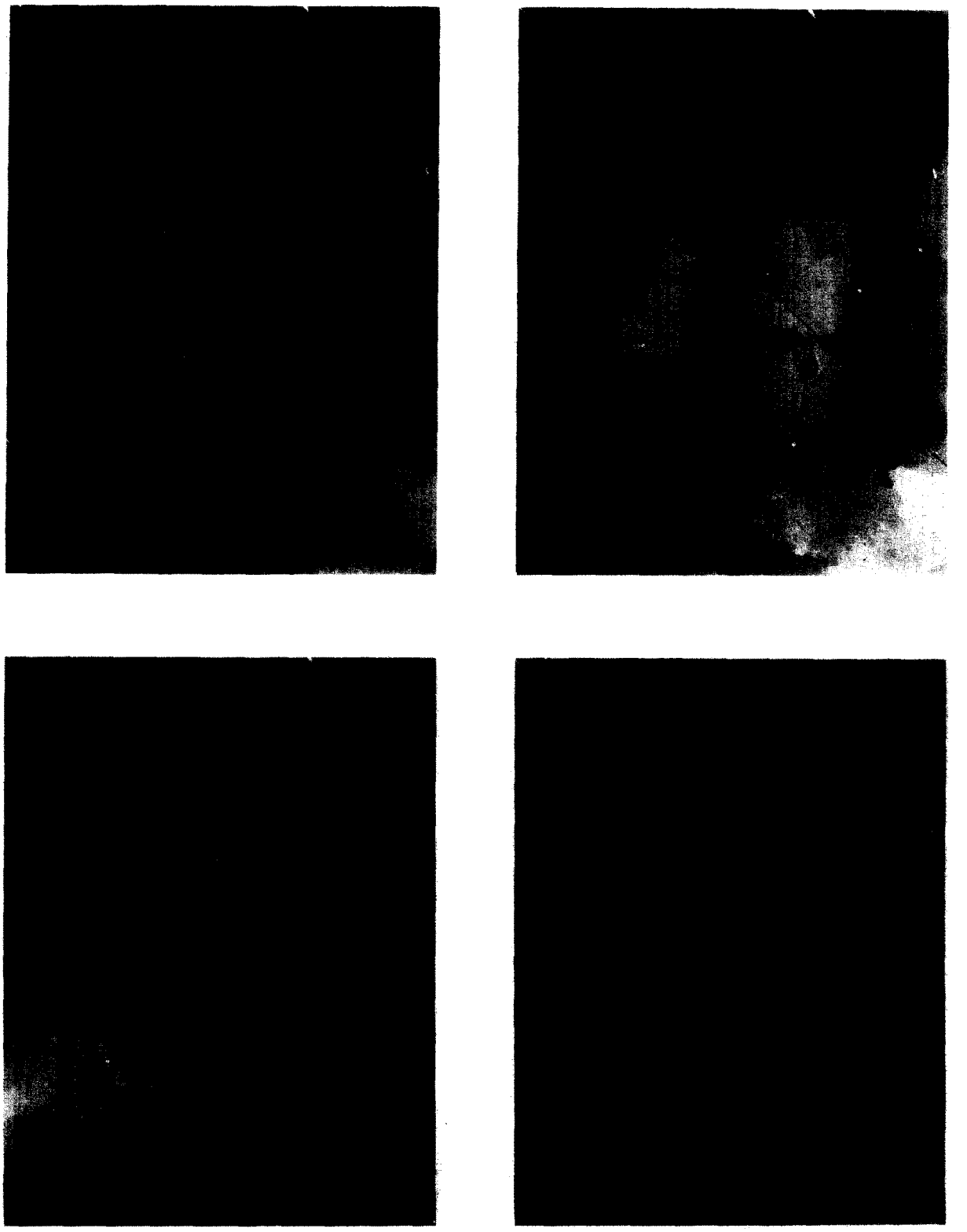

FIG. 2. The series of photomicrographs shows the total extinction of all individual crystals within ±2°. The angles of the individual photos are: 2a: 35.4°, 2b: 36.0°, 2c: 36.2°, 2d: 37.8°. The long dimension of the photos is 3.6 mm; crossed nicols.

negative crystals, about 5–10 μm in size, have vapor/liquid volumetric ratios that typically range from 5–10%, and contain water-vapor bubbles. They are either associated with the formation of the quartz or with a severe metamorphic event. Figure 3a–b shows several examples of primary fluid inclusions. Secondary inclusions occur along crystal defects or

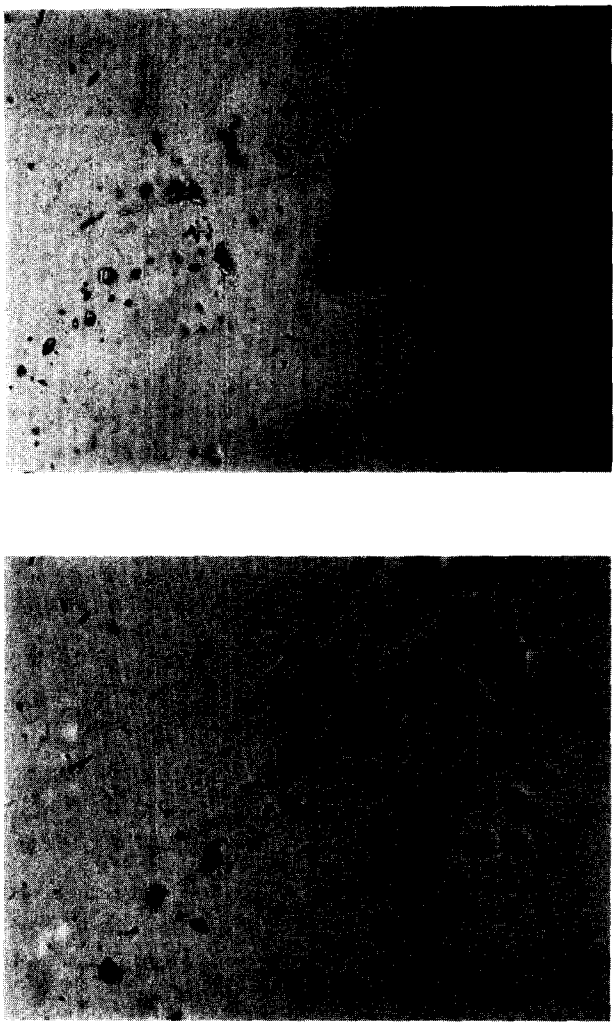

FIG. 3. Fluid inclusions within a thin section of quartz from the Roter Kamm crater. There is no obvious connection of the distribution of the fluid inclusions with domain boundaries (3a). The size of most primary inclusions (which are often in the shape of negative crystals and contain a water vapor bubble) is 5–10 μm. Long dimensions of the photos: 3a: 0.62 mm, 3b: 0.31 mm. At the higher magnification the very small secondary inclusions are also visible. Crossed nicols, green filter.

grain boundaries and are usually smaller than 1 μm and were thus too small for further studies. In addition, there are a few late (recent?) large (10 μm or larger) fluid inclusions of irregular shape, which are in some cases associated with fractures.

We have studied the primary fluid inclusions in a thick section (120 μm thickness) that was specifically made for this purpose. The freezing point depressions indicate salinities (determined from experimental $NaCl/H_2O$ data given by POTTER *et al.*, 1978; and POTTER and CLYNNE, 1978) ranging between 18.3 and 19.6 wt% $NaCl_{eq}$ for most inclusions (with freezing points ranging from −14.5 to −16°C). These salinities are higher than most of the salinities determined by KOMOR *et al.* (1988a,b) for fluid inclusions in quartz at the Siljan impact structure and by BAIN and KISSIN (1988) for fluid inclusions in glasses of polymict breccias at the Haughton impact structure, which can be understood in terms of the different geological setting of these impact structures.

Homogenization temperatures (T_h) have been measured for a number of inclusions and range between 165 and 250°C with a maximum between 200 and 210°C. Figure 4 gives a histogram of the homogenization temperatures for the primary fluid inclusions in the Roter Kamm quartz. Decrepitation of some fluid inclusions was observed at temperatures of 220°C and higher. These temperatures are higher than the ones observed by BAIN and KISSIN (1988) in glass from the Haughton impact structure, but compatible or even lower than the ones observed by KOMOR *et al.* (1988a,b) in quartz from the Siljan impact structure.

Studies of fluid inclusions in the quartz crystals from the pegmatites show a distinctly different picture. In sections of the cloudy white quartz we have not seen any primary inclusions, only very small (<0.5 μm) inclusions which are too small to be studied. In addition, there are very few small (<2 μm) secondary inclusions, and a few late irregular inclusions (filled with only liquid, no vapor). The clear quartz contains many different types of solid (*e.g.*, chloride) and fluid inclusions: one type of primary inclusion, up to 10 μm, has salinities between 20.4 and 21.2 wt% $NaCl_{eq}$ and homogenization temperatures up to 290°C. A few slightly larger primary inclusions show decreasing salinities between 17 and 18.8 wt% $NaCl_{eq}$ and t_h of about 210°C. Numerous, very small secondary inclusions are abundant in trails. Some of them are characterized by T_h's lower than 160°C and salinities of less than 11.7 wt% $NaCl_{eq}$, while others are too small to allow measurements. The abundance and distribution of inclusions in the pegmatite quartz is unlike in the quartz pebbles.

DISCUSSION AND CONCLUSIONS

It is not possible to date the fluid inclusions absolutely or in respect to the host quartz because there are no obvious shock deformation features with associated fluid inclusions in the quartz. We suggest, however, that the majority of the fluid inclusions have been formed during a post-impact hydrothermal event. The quartz has probably grown from or recrystallized in the hydrothermal fluids. High salinity liquids in inclusions are usually thought to be indicative of fluids released by silica-rich magmas, while low salinity liquids are more commonly observed from meteoric waters. The rather high salinity of the fluid inclusions in the Roter Kamm quartz

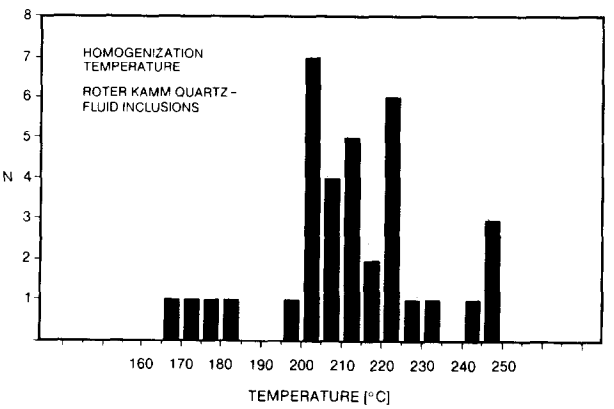

FIG. 4. Histogram of the homogenization temperatures (T_h) of the primary fluid inclusions within quartz from the Roter Kamm crater. The average T_h is between 200 and 210°C.

may result from high salinity water released by the basement gneisses and pegmatites during the impact. The released water then formed a hydrothermal circulation system within the crater. The homogenization temperatures of the fluid inclusions are in a range that is compatible with an origin in a hydrothermal event. KOMOR *et al.* (1988a) note that homogenization temperatures of 165 to 309°C are indicative of the precipitation of quartz by impact-generated hydrothermal mineral solutions.

Hydrothermal activity has been documented at several terrestrial impact structures in layers above and below the melt sheets. Impact melts and breccias have been altered in some cases by hydrothermal fluids to clays, potassium feldspar, and quartz, indicating fluid temperatures of about 100 to 300°C (ALLEN *et al.*, 1982). Studies of mineral alterations at West Clearwater Lake (PHINNEY *et al.*, 1978) and the Ries crater (NEWSON *et al.*, 1987) indicate temperatures >500°C, while the hydrothermal assemblages in impact products at the Rochechouart impact structure (REIMOLD *et al.*, 1987) suggest temperatures of ~700°C associated with the formation of pseudotachylite. The small size of the Roter Kamm impact crater and the smaller amount of impact heat associated with its formation compared to the larger impact structures discussed by ALLEN *et al.* (1982), NEWSOM *et al.* (1987), BAIN and KISSIN (1988) and KOMOR *et al.* (1988a,b) is in agreement with the fluid temperatures indicated by the fluid inclusion homogenization temperatures.

Because there are no signs of any geological/igneous activity in the area between about 900 Ma (the age of the target rock formation) and the formation of the crater, it seems plausible (as indicated by the structure, occurrence, and homogenization temperatures of the fluid inclusions) to conclude that hydrothermal activity was responsible for the formation of the fluid inclusions in the quartz. In addition, a study of fluid inclusions in the target material (quartz from quartz pegmatites), has demonstrated that there are significant differences between the quartz pebbles thought to have formed during post-impact hydrothermal activity and the target rock quartz crystals. The microscopic appearance, the occurrence, content, and distribution of fluid inclusions, and the H_2O and CO_2 contents are distinctly different. This supports the interpretation of the quartz pebbles as evidence for post-impact hydrothermal activity.

After an impact, a boiling water table forms below the impact melt sheet (which in the case of the Roter Kamm crater most probably was not continuous), and steam and water escape mainly at the crater rim (or, if it is a complex impact structure, also at the central uplift), while the circulation through the actual melt sheet is minimal (NEWSOM, 1980). The lifetime of the hydrothermal circulation system at larger craters may be up to several thousand years (NEWSOM, 1980), while for the Roter Kamm crater it may be less than a few hundred years. In conclusion, we suggest that the anomalous quartz found at the rim of the crater, and the primary fluid inclusions in the quartz, seem to provide evidence for post-impact hydrothermal activity, generated by impact heat, at the Roter Kamm impact crater.

Acknowledgements—We are grateful to P. Dunn and D. Appleman (Department of Mineral Sciences, Smithsonian Institution) for the X-ray diffraction analysis, and to R. Johnson and F. Walkup (Smithsonian Institution) for exacting thin sections. We would also like to acknowledge the support of R. McG. Miller (Geological Survey of SWA/Namibia, Windhoek) for extensive support during the field work. We are indebted to J. B. Garvin, E. Roedder, and an anonymous reviewer for their detailed comments on the manuscript. We thank Dona Jalufka for artwork. This study was supported by the Austrian Fonds zur Förderung der Wissenschaftlichen Forschung (FFWF), project No. P6072 E. The Lunar and Planetary Institute is operated by the Universities in Space Research Association under contract NASW-4066 with the National Aeronautics and Space Administration. This is Lunar and Planetary Institute Contribution No. 715.

Editorial handling: G. Faure

REFERENCES

ALLEN C. G., GOODING J. L. and KEIL K. (1982) Hydrothermally altered impact melt rock and breccia: Contributions to the soil of Mars. *J. Geophys. Res.* **87**, 10083–10101.

BAIN J. G. and KISSIN S. A. (1988) A preliminary study of fluid inclusions in shock-metamorphosed sediments at the Haughton impact structure, Devon Island, Canada. *Meteoritics* **23**, 256.

BISHOP J., KOEBERL C. and REIMOLD W. U. (1989) Geochemistry of the Roter Kamm impact crater, SWA/Namibia. In *Proc. 52nd Annual Meeting of the Meteoritical Society, Vienna* (in press).

DIETZ R. S. (1965) Roter Kamm, South West Africa: Probable meteorite crater. *Meteoritics* **2**, 311–314.

FUDALI R. F. (1973) Roter Kamm: Evidence for an impact origin. *Meteoritics* **8**, 245–257.

KOMOR S. C., VALLEY J. W. and BROWN P. E. (1988a) Fluid-inclusion evidence for impact heating at the Siljan Ring, Sweden. *Geology* **16**, 711–715.

KOMOR S. C., VALLEY J. W., BROWN P. E. and COLLINI B. (1988b) Fluid inclusions in granite from the Siljan Ring impact structure and surrounding regions. In *Deep Drilling in Crystalline Bedrock*, Vol. 1 (eds. A. BODEN and K. G. ERIKSSON), pp. 180–208. Springer Verlag, Berlin.

MILLER R. McG. and REIMOLD W. U. (1986) Deformation and shock deformation in rocks at the Roter Kamm crater, SWA/Namibia. *Meteoritics* **21**, 456–458.

NEWSOM H. E. (1980) Hydrothermal alteration of impact melt sheets with implications for Mars. *Icarus* **44**, 207–216.

NEWSOM H. E., GRAUP G., SEWARDS T. and KEIL K. (1987) Fluidization and hydrothermal alteration of the suevite deposit at the Ries crater, West Germany, and implications for Mars. *Proc. Lunar Planet. Sci. Conf. 17th; J. Geophys. Res.* **91**, E239–E251.

PHINNEY W. C., SIMONDS C. H., COCHRAN A. and McGEE P. E. (1978) West Clearwater, Quebec impact structure, Part II: Petrology. *Proc. Lunar Planet. Sci. Conf. 9th*, 2659–2694.

POTTER R. W., II and CLYNNE M. A. (1978) Solubility of highly soluble salts in aqueous media—Part 1: NaCl, KCl, $CaCl_2$, Na_2SO_4 and K_2SO_4 solubilities to 100°C. *J. Res. U.S. Geol. Surv.* **6**, 701–705.

POTTER R. W., II, CLYNNE M. A. and BROWN D. L. (1978) Freezing point depressions of aqueous sodium chloride solutions. *Econ. Geol.* **73**, 284–285.

REIMOLD W. U. and MILLER R. McG. (1987) Roter Kamm crater, SWA/Namibia. In *Excursion Guide to the Gross Brukkaros and Roter Kamm Craters, SWA/Namibia* (eds. R. McG. MILLER and W. U. REIMOLD). Univ. of the Witwatersrand, Johannesburg.

REIMOLD W. U. and MILLER R. McG. (1989) The Roter Kamm impact crater, SWA/Namibia. *Proc. Lunar Planet. Sci. Conf. 19th*, pp. 711–732.

REIMOLD W. U., OSKIERSKI W. and HUTH J. (1987) The pseudotachylite from Champagnac in the Rochechouart meteorite crater, France. *Proc. Lunar Planet. Sci. Conf. 17th, J. Geophys. Res.* **92**, E737–E748.

REIMOLD W. U., MILLER R. McG., GRIEVE R. A. F. and KOEBERL C. (1988) The Roter Kamm crater structure in SWA/Namibia. *Lunar Planet. Sci.* **XIX**, 972–973.

SCHWARZMAN E. C., MEYER C. E. and WILSHIRE H. G. (1983) Pseudotachylite from the Vredefort Ring, South Africa, and the origins of some lunar breccias. *Geol. Soc. Amer. Bull.* **94**, 926–935.

THOMPSON W. K. (1965) Infra-red spectroscopic studies of aqueous systems. *Trans. Faraday Soc.* **61**, 1635–1640.